Integrated all-optical MIMO demultiplexer for mode- and wavelength-division-multiplexed transmission

Daniele Melati,[1,*] Andrea Alippi,[1,2] Andrea Annoni,[1] Nicola Peserico,[1] and Andrea Melloni[1]

[1]Dipartimento di Elettronica, Informazione e Bioingegneria, Politecnico di Milano, via Ponzio 34/5, 20133 Milano, Italy

[2]Currently at Linkra Microtech, 20864 Agrate Brianza, Italy

*Corresponding author: daniele.melati@polimi.it

A photonic integrated circuit performing simultaneous mode and wavelength demultiplexing for few-mode-fiber transmission is demonstrated for the first time. The circuit is realized on an InP-based technological platform; it can handle up to eight mode- and wavelength-division-multiplexed (MDM/WDM) channels and allows all-optical multiple-input-multiple-output processing to unscramble mode mixing generated by fiber propagation. A single ar-rayed waveguide grating is used to demultiplex the WDM channels carried by all the propagating modes, optimizing circuit complexity, chip area, and operational stability. Combined with an integrated wideband mode multiplexer the circuit is successfully exploited for the transmission of 10 Gbit⁄s on-off-keying non-return-to-zero channels with a residual cross talk of about −15 dB

Wavelength-division multiplexing (WDM) is nowadays a core element of many optical transmission systems enabling large fiber capacity compared to single-wavelength links. Likewise, the possibility to add space multiplexing capabilities in the transmission systems is regarded as a viable and promising approach for the future to further improve spectral efficiency [1], providing a solution to overcome the fast-approaching limit of single-mode fiber transport capacity [2,3]. Remarkably, recent experiments demonstrating ultrahigh-density multiplexing and Pbit/s transmission capacity commonly rely on hybrid space- and wavelength-multiplexed links [4,5]. Among the different space multiplexing technologies, mode-division multiplexing (MDM) over few-mode fibers (FMFs) is a widely investigated option for simultaneous transmission of light paths over different modes [6]. The use of multiple modes introduces, on the other hand, the problem of mode cross talk since in many cases power can be coupled from one propagating mode to another, causing linear mixing of the signals carried by the modes [7–9]. Multiple-input-multiple-output (MIMO) demultiplexing is hence necessary to unmix signals at the receiver and this is generally done through electronic digital signal processors [10]. However, this solution could be power hungry andcomplexfor high symbol-rate or many propagating modes. Alternatively, all-optical MIMO demultiplexing is insensitive to symbol rate and reduces power consumption required to unscramble and track propagating modes, at least in low-dispersion links with negligible differential group delay [7,8,11].

In this scenario, photonic integrated circuits can provide a compact and scalable approach to include mode diversity in transmission systems [11]. However, to be suitable for advanced communication schemes, these circuits must be able to handle hybrid MDM/WDM transmissions. For example, some integrated mode couplers compatible with WDM transmission have been recently proposed [12,13] as well as integrated WDM filters operating on different modes simultaneously [14]. In this Letter, we propose and experimentally demonstrate for the first time, to our knowledge, a photonic integrated cir-cuit for short-reach few-mode-fiber transmission performing simultaneous mode and wavelength demultiplexing. The cir-cuit design exploits a single arrayed waveguide grating (AWG) for wavelength demultiplexing, optimizing complexity, size, and operational stability. Moreover, the mode demultiplexing stage integrates all-optical MIMO processing capabilities to unscramble mode mixing generated by fiber propagation. MDM/WDM demultiplexing and mode-mixing unscramble are demonstrated after propagation in a few-meter long FMF, reaching a residual channel cross talk of about −15 dB on 10 Gbit/s on-off-keying (OOK) non-return-to-zero (NRZ) channels transmitted through an integrated wideband mode multiplexer [13].

Figures 1(a) and 1(b) show the schematic of the mode and wavelength demultiplexer and the photograph of the device fabricated through a JePPIX Multi-Project Wafer Run [15] on an InP-based technological platform. The exploited wave-guide is rib-shaped with 1 μm thick InGaAsP core on top of the InP substrate, etch depth of 1.7 μm and no top cladding.

Received 21 November 2016;
revised 15 December 2016;
accepted 15 December 2016;
posted 16 December 2016 (Doc. ID 281031);
published 12 January 2017

OCIS codes: (130.3120) Integrated optics devices; (130.7408) Wavelength filtering devices; (060.4230) Multiplexing; (060.2330) Fiber optics communications.

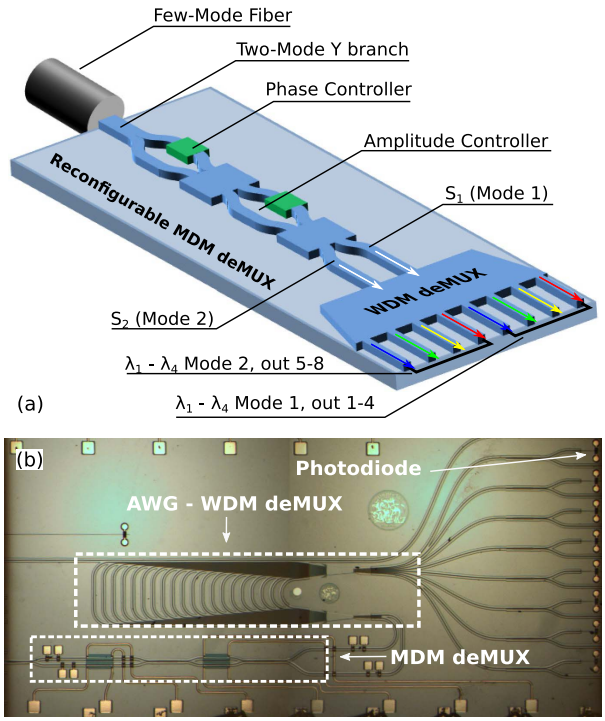

Fig. 1. (a) Schematic of the integrated mode and wavelength demultiplexer. (b) Photograph of the realized circuit.

The circuit has a single input two-mode waveguide that can be directly coupled to a 11 μm core FMF [16] and receives modes LP_{01} and LP_{11a} with up to four WDM channels per mode with 50 GHz spacing. An adiabatic taper maximizes power coupling up to an efficiency of −6 dB with 1 dB mode-dependent losses. The 2×4 MDM/WDM channels are demultiplexed to the eight single-mode output waveguides of the circuit, equipped also with integrated photodiodes. The circuit comprises two cascaded stages. The first one is the wideband mode demultiplexer previously proposed in [13]. This stage is based on a reconfigurable linear network and intrinsically integrates all-optical MIMO capabilities [17,18]. The fundamental mode of the input waveguide is excited by the LP_{01} mode of the fiber while mode LP_{11a} couples on the first-higher-order mode of the waveguide. A symmetric Y-branch converts the fundamental and first-order mode of the two-mode input waveguide into the fundamental modes of two separated single-mode waveguides. After the Y-branch, the linear network controls the coupling between the two outputs of the Y-branch and the waveguides S_1 and S_2 at the output of the mode demultiplexing stage [Fig. 1(a)]. The network includes a phase shifter to adjust the relative phase between the two branches of the network (phase controller) and a balanced Mach–Zehnder interferometer as amplitude controller. Both are based on thermo-optic actuators ($V_\pi = 4.8$ V). When the phase controller is turned off and a voltage of 3.1 V is fed to the amplitude controller, the input mode LP_{01} is completely mapped on the fundamental mode of waveguide S_1. Likewise, input mode LP_{11a} is coupled to waveguide S_2. The mapping can be reversed, for example, by applying a π shift to the phase controller (voltage 4.8 V), to direct mode LP_{11a} to S_1 and LP_{01} to S_2. The same operation can be done with any linear combination of the FMF modes at the circuit input, enabling all-optical MIMO demultiplexing as described in the next section.

The second cascaded stage is a WDM demultiplexer realized by means of a single eight-channel AWG with twice the free spectral range (FSR) required to accommodate the four WDM channels. The AWG has two inputs (directly connected to S_1 and S_2) and eight outputs with channel spacing of 50 GHz, FSR of 400 GHz, and central wavelength of 1550 nm. The AWG cross-talk suppression between wavelength channels measured on an isolated device is about 20 dB for both input ports. The position of the input ports was designed in order to have the two transfer functions from S_1 and S_2 to output ports shifted exactly of half the FSR of the AWG. The wavelength range of 200 GHz (1.6 nm) is the actual bandwidth exploited by the circuit to accommodate the four WDM channels, much narrower than the bandwidth of the mode demultiplexer. Wavelengths λ_1–λ_4 at S_1 are demultiplexed at output ports 1–4; the same wavelengths entering from S_2 are demultiplexed at output ports 5–8. With this configuration, a single AWG (instead of two) can be used as WDM demultiplexer for both input modes, reducing the circuit complexity and the required chip area while improving operational stability. At the eight outputs of the AWG, 3 dB couplers allow to collect the demultiplexed channels through either a standard lensed fiber or the integrated photodiodes.

The described circuit was exploited to demultiplex MDM/WDM channels after propagation in a 2 m long graded-index FMF with a core width of 11 μm and differential group delay of about 0.08 ps/m [16], ensuring an almost frequency-independent mode cross talk and negligible total differential group delay between the propagating modes [11]. TE-polarized fiber modes were excited by cascading a tunable laser source, a polarization controller, and the integrated wideband mode multiplexer described in [13], hence exploiting integrated circuits at both transmitter and receiver sides. Similar results were obtained by exciting TM modes. The controllers of the mode multiplexer allowed to selectively excite either mode LP_{01} or LP_{11a} in the FMF with a mode cross talk of about −20 dB. Angular alignment of the fiber to both the multiplexer and demultiplexer was carefully controlled in order to ensure good coupling between mode LP_{11a} and the first-order waveguide mode. The demultiplexer was set in order to map mode LP_{01} to waveguide S_1 and mode LP_{11a} on S_2. Figure 2 shows the normalized transfer functions of the system at the demultiplexer optical outputs for both fiber modes measured by means of an optical spectrum analyzer synchronized with the tunable laser source. The clear areas in the graphs highlight the 1.6 nm wavelength ranges that can be exploited (half of the FSR of the AWG) while the gray areas correspond to the spectral portions that cannot be used (wavelengths λ_5–λ_8). Areas are spectrally separated by a full FSR (3.2 nm). When mode LP_{01} is injected at the input waveguide of the demultiplexer, the four wavelength channels between, for example, 1551.8 and 1553 nm are demultiplexed at output ports 1–4 [Fig. 2(a)]. As expected, the output ports 6 and 8 are isolated, with an extinction between 10 and 15 dB [Fig. 2(b)]. Unfortunately, output ports 5 and 7 were damaged on the available sample and could not be measured but similar results are expected. The residual mode channel cross talk is comparable with single-wavelength MDM transmission exploiting the integrated mode multiplexer and demultiplexer [13]. Transmission is quite uniform across the

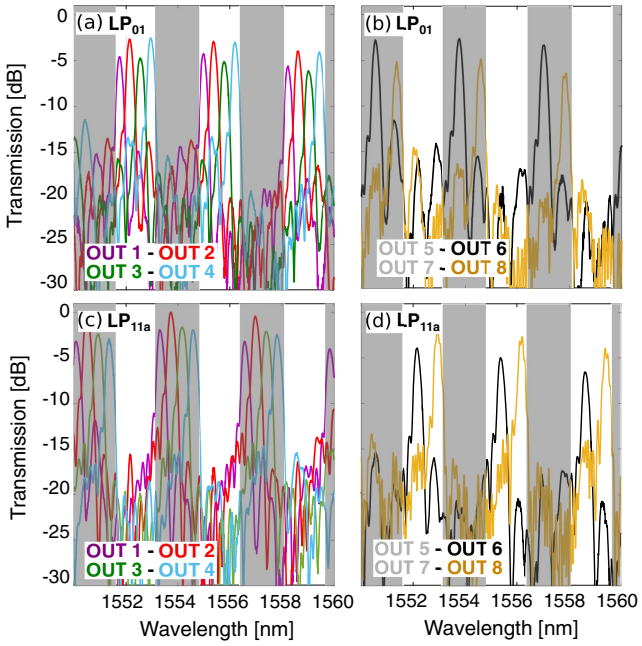

Fig. 2. Measured transfer functions at the eight output ports of the demultiplexer while injecting (a) and (b) mode LP_{01} or (c) and (d) mode LP_{11a}.

channels, with fluctuations of the order of 2 dB. Circuit operation is reversed when mode LP_{11a} is coupled at the input, as shown in Figs. 2(c) and 2(d). In this case output ports 1–4 are isolated while wavelengths between 1551.8 and 1553 nm are demultiplexed at output ports 5–8. The residual mode channel cross talk is again of the order of about −15 dB. Obviously, if the considered wavelength range is shifted by 1.6 nm, S_1 and S_2 transfer functions are swapped.

Besides switching purposes [13], the reconfiguration capability of the MDM stage can be exploited to perform all-optical MIMO processing for mode unscrambling. This was demonstrated using the mode multiplexer to intentionally introduce mode mixing in a controlled manner, mimicking the effect generated by a long fiber propagation. We considered as an example the transmission of mode LP_{01} and monitored the demultiplexed output 6. Figure 3(a) shows the normalized transmission for one of the 1.6 nm available wavelength ranges (clear area). The reference condition (gray solid curve) is the same shown in Fig. 2(b), corresponding to a quite pure LP_{01} excitation in the FMF, with power transmitted on the LP_{11a} mode lower than −20 dB compared to LP_{01} power. As expected, in this case output 6 is isolated (about −15 dB) since LP_{01} mode is demultiplexed at outputs 1–4 [see Fig. 2(a)]. Acting on the mode multiplexer we then excited a mixture of modes LP_{01} and LP_{11a}, progressively increasing the power coupled to the latter and reducing consequently the power on mode LP_{01} (keeping constant the total transmitted power). This situation is equivalent to pure LP_{01} excitation at the mode multiplexer but having part of the power coupled to mode LP_{11a} during fiber propagation. As can be seen (dotted red curve and dashed blue curve), the increase of the relative amount of power on mode LP_{11a} reduces the isolation of port 6. For the dotted red curve the ratio between LP_{01} and LP_{11a} power at the output of the mode multiplexer was estimated

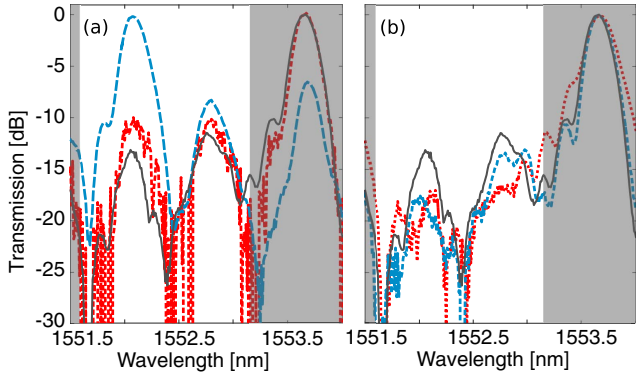

Fig. 3. Transmission at output 6 in the reference case (pure LP_{01} transmission, gray solid curve) and introducing mode mixing (dotted red curve and dashed blue curve). (a) Results without MIMO processing and (b) exploiting controllers of the mode demultiplexing stage to perform mode unscrambling.

between −5 and −10 dB and isolation of output 6 of the demultiplexer reduces consequently, increasing mode channel cross talk. In the case of the dashed blue curve, the power transmitted on mode LP_{11a} was higher than that coupled on mode LP_{01}, with the same estimated ratio at the mode multiplexer (5 to 10 dB). Most of the power was hence demultiplexed at output 6, which was intended to be an isolated port. In order to compensate the induced mode channel cross talk we exploited the controllers available on the MDM demultiplexing stage and results are shown in Fig. 3(b). For the dotted red curve, 3.1 V and 2.8 V were fed to the amplitude and phase controllers, respectively. In the case of the dashed blue curve, the phase controller was turned off while amplitude was controlled with a voltage of 4.7 V. In both cases it was possible to reconstruct the desired circuit operation with isolated output 6. The residual mode channel cross talk is even lower than the reference case that was probably affected also by a slight mode mixing generated by the fiber or by fiber–chip interfaces, compensated through the optimized settings of the demultiplexer.

The proposed demultiplexer was finally tested within the MDM/WDM transmission systems sketched in Fig. 4. In the first case [Fig. 4(a)] two independent 10 Gbit/s OOK NRZ channels were generated at $\lambda_2 = 1558.1$ nm and $\lambda_4 = 1558.9$ nm. After amplification and polarization adjustment, channels were coupled to the integrated mode multiplexer [13]

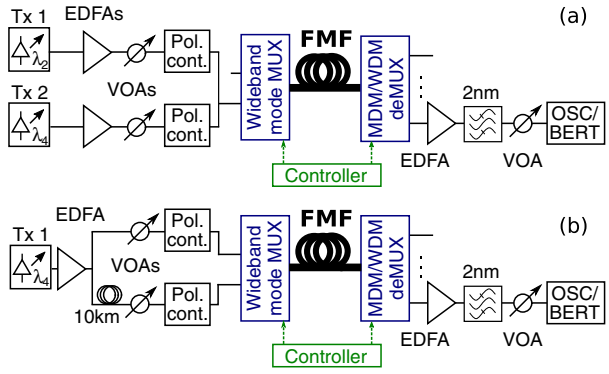

Fig. 4. Experimental setup for two-channel 10 Gbit/s OOK NRZ transmission exploiting (a) two wavelengths and (b) two modes.

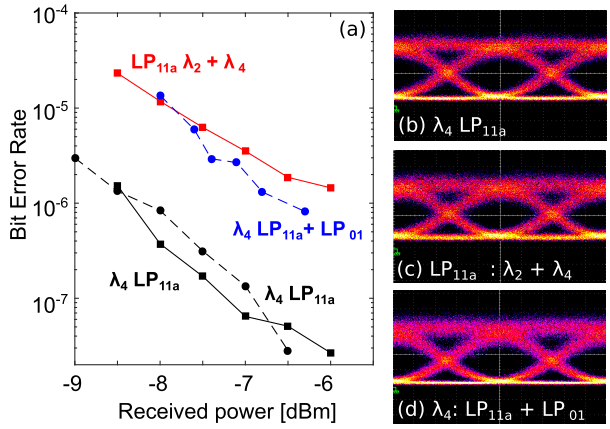

Fig. 5. Transmission results. (a) Bit-error rate and (b)–(d) corresponding eye diagrams when one channel (black curves) and two channels are simultaneously transmitted.

(highlighted in blue) to be transmitted on mode LP_{11a}. At the receiver side, the channel grid of the MDM/WDM demultiplexer (highlighted in blue) was aligned to the transmitted wavelengths by a Peltier element placed in the chip holder. The set point of the circuit was the same described before and mode LP_{11a} was hence demultiplexed at output ports 5–8. The channel at λ_4 was collected optically at output port 8 and sent into either an optical oscilloscope or bit-error rate (BER) tester after amplification and filtering. Figure 5(a) shows with solid lines the BER measurements as a function of the received power. Compared to the reference performance (λ_2 switched off, black solid curve), the power penalty is about 2.5 dB at a BER level of $1.5 \cdot 10^{-6}$ (red solid curve). The corresponding eye diagrams with λ_2 either switched off or switched on are shown in Figs. 5(b) and 5(c). As can be seen, a good eye-opening is preserved with only a small degradation on the second eye diagram when compared to single channel transmission due to the residual cross talk. The measured eye Q-factor reduces from 6.3 (single channel) to 5.2 (double channel). In the second experiment, sketched in Fig. 4(b), the two independent channels were generated at the same wavelength $\lambda_4 = 1558.9$ nm exploiting a 10 km long fiber coil for decorrelation and simultaneously transmitted over the two modes LP_{01} and LP_{11a} by means of the mode multiplexer. At the receiver, mode LP_{01} was demultiplexed at port 4 while LP_{11a} at port 8. The latter was collected and sent to the oscilloscope and BER tester. Figure 5(a) shows the BER measurements with dashed lines. In this case the power penalty is about 1.7 dB (blue dashed curve) compared to the reference performance at BER of $1.5 \cdot 10^{-6}$ with mode LP_{01} switched off (black dashed line). As in the previous case, the corresponding eye diagram shown in Fig. 5(d) is only slightly degraded compared to single-channel transmission [Fig. 5(b)] and the Q-factor reduces to 5.3.

In conclusion, we have demonstrated for the first time, to our knowledge, a photonic integrated circuit performing both mode and wavelength demultiplexing for FMF transmission. The circuit can handle up to two MDM channels and four WDM channels per mode. The mode demultiplexing stage integrates a reconfigurable linear network that enables all-optical MIMO processing to unscramble mode mixing. The design of the WDM filter allows use of a single AWG for the signals carried by both MDM channels, optimizing complexity, size, and operational stability. Channel demultiplexing was demonstrated with a residual cross talk of about −15 dB. This cross-talk level was reached and improved also with the mode mixing intentionally introduced at the transmitter side, mimicking the effect generated by fiber propagation. All-optical MIMO processing could be automated by implementing, for example, the technique described in [19] to provide adaptive compensation of environmental fluctuations. Lastly, simultaneous transmission of two 10 Gbit/s NRZ OOK channels was demonstrated exploiting either two different modes or two different wavelengths, with a power penalty of about 2 dB on BER measurements and negligible eye diagrams distortion. The described circuit could be extended to demultiplex more than two mode channels by implementing a larger reconfigurable linear network [18] and an AWG with a consistent number of output channels, relying, for example, on vertical coupling [20] for FMF interfacing.

REFERENCES

1. P. J. Winzer, Nat. Photonics **8**, 345 (2014).
2. A. D. Ellis, J. Zhao, and D. Cotter, J. Lightwave Technol. **28**, 423 (2010).
3. D. J. Richardson, J. M. Fini, and L. E. Nelson, Nat. Photonics **7**, 354 (2013).
4. R. G. van Uden, R. A. Correa, E. A. Lopez, F. M. Huijskens, C. Xia, G. Li, A. Schülzgen, H. de Waardt, A. M. Koonen, and C. M. Okonkwo, Nat. Photonics **8**, 865 (2014).
5. K. Igarashi, D. Soma, Y. Wakayama, K. Takeshima, Y. Kawaguchi, N. Yoshikane, T. Tsuritani, I. Morita, and M. Suzuki, Opt. Express **24**, 10213 (2016).
6. J. van Weerdenburg, A. Velàzquez-Benitez, R. van Uden, P. Sillard, D. Molin, A. Amezcua-Correa, E. Antonio-Lopez, M. Kuschnerov, F. Huijskens, H. de Waardt, T. Koonen, R. Amezcua-Correa, and C. Okonkwo, Opt. Express **23**, 24759 (2015).
7. C. R. Doerr, IEEE Photon. Technol. Lett. **23**, 1573 (2011).
8. N. K. Fontaine, *Optical Fiber Communication Conference/National Fiber Optic Engineers Conference* (Optical Society of America, 2013).
9. E. Ip, M. J. Li, W. Wood, J. Hu, and Y. Yano, *IEEE Photonics Society Summer Topical Meeting Series* (IEEE, 2013).
10. R. Ryf, M. A. Mestre, S. Randel, C. Schmidt, A. H. Gnauck, R.-J. Essiambre, P. J. Winzer, R. Delbue, P. Pupalaikis, A. Sureka, Y. Sun, X. Jiang, D. W. Peckham, A. McCurdy, and R. Lingle, IEEE Photon. Technol. Lett. **24**, 1965 (2012).
11. N. K. Fontaine, C. R. Doerr, M. A. Mestre, R. Ryf, P. Winzer, L. Buhl, Y. Sun, X. Jiang, and R. Lingle, *Optical Fiber Communication Conference* (Optical Society of America, 2012).
12. H. Chen, V. Sleiffer, B. Snyder, M. Kuschnerov, R. van Uden, Y. Jung, C. M. Okonkwo, O. Raz, P. O'Brien, H. de Waardt, and T. Koonen, IEEE Photon. Technol. Lett. **25**, 2039 (2013).
13. D. Melati, A. Alippi, and A. Melloni, Opt. Express **24**, 12625 (2016).
14. H. Chen, N. K. Fontaine, B. Guan, B. Ercan, Y. Zhang, R. Ryf, M. Cappuzzo, B. Keller, Y. Gao, C. Ferrari, R. P. Scott, and S. J. B. Yoo, *European Conference on Optical Communication* (IEEE, 2015).
15. JePPIX, http://www.jeppix.eu.
16. L. Gruner-Nielsen, Y. Sun, J. Nicholson, D. Jakobsen, K. G. Jespersen, R. Lingle, and B. Palsdottir, J. Lightwave Technol. **30**, 3693 (2012).
17. D. A. B. Miller, Opt. Express **21**, 20220 (2013).
18. F. Morichetti, A. Annoni, S. Grillanda, N. Peserico, M. Carminati, P. Ciccarella, G. Ferrari, E. Guglielmi, M. Sorel, and A. Melloni, *Optical Fiber Communication Conference* (Optical Society of America, 2016).
19. A. Annoni, E. Guglielmi, M. Carminati, S. Grillanda, P. Ciccarella, G. Ferrari, M. Sorel, M. J. Strain, M. Sampietro, A. Melloni, and F. Morichetti, IEEE J. Sel. Top. Quantum Electron. **22**, 169 (2016).
20. H. Chen, R. van Uden, C. Okonkwo, and A. Koonen, Opt. Express **22**, 31582 (2014).